SCIPEDIA

ANN-based surrogate model for predicting the lateral load capacity of RC shear walls

German Solorzano Solorzano[1], Vagelis Plevris Plevris[2]

[1] Oslo Metropolitan University
[2] Qatar University

ANN-BASED SURROGATE MODEL FOR PREDICTING THE LATERAL LOAD CAPACITY OF RC SHEAR WALLS

GERMAN SOLORZANO[1] AND VAGELIS PLEVRIS[2]

[1] Department of Civil Engineering and Energy Technology
OsloMet–Oslo Metropolitan University
Pilestredet 35, Oslo 0166, Norway
e-mail: germanso@oslomet.no

[2] Department of Civil and Architectural Engineering
Qatar University
P.O. Box: 2713, Doha, Qatar
e-mail: vplevris@qu.edu.qa

Key words: Shear Wall, Surrogate Model, Neural Network, OpenSees, Finite Element, Lateral Load Capacity

Abstract. Reinforced concrete (RC) shear walls are often used as the main lateral-resisting component in the seismic design of buildings. They provide a large percentage of the lateral stiffness of the structure, and therefore, they may experience large shear stresses at some point under earthquake loading. Consequentially, to accurately predict their behavior, it is recommended to use detailed finite element (FE) modeling with appropriate non-linear constitutive models for concrete and steel. However, such types of simulations are challenging and could significantly increase the computational time required to obtain the analysis results. In this paper, we study the viability of creating an artificial neural-network-based surrogate model of the RC shear wall that is able to capture its nonlinear behavior and predict the results obtained with a detailed FE model, offering a much lower computational effort. For this purpose, we develop a detailed parametric non-linear FE model based on well-established practices and validated studies using the OpenSees finite element software framework. The FE model consists of multi-layer shell elements with the vertical and transverse reinforcement included as smeared rebar layers. The concrete layers implement a damage mechanism with smeared crack constitutive model, whereas the rebar layers consider a uniaxial plasticity material law. The parametric FE model is used to build a large database of RC walls of different sizes and characteristics, with their corresponding lateral load capacity that is obtained through the detailed non-linear pushover analysis. Finally, the obtained database is used to train and validate the ANN-surrogate model. The developed model is able to accurately predict the lateral load capacity of RC shear walls without the need of detailed FE modeling, thus drastically reducing the complexity and the computational time required for the numerical solution and providing a reliable and robust analysis alternative, with only small compromise of accuracy.

1 INTRODUCTION

Reinforced concrete (RC) shear walls are one of the most commonly used structural systems in the seismic design of buildings. They provide most of the lateral stiffness, and consequentially, they may experience extremely large shear forces during earthquakes [1]. As a result, their properties and behavior have been subject of numerous studies, including rigorous experimental tests [2, 3, 4], and thorough investigations on how to properly include them in Finite Element (FE) simulations. This has resulted in various modeling techniques ranging from simple shear spring systems [5, 6, 7] to more sophisticated models using shell and solid elements [8, 9, 10]. However, it is well known that the mathematical modeling of reinforced concrete under extreme loading conditions is a challenging endeavour, mainly due to the complex mechanisms involved in the structural behavior, such as the cracking or crushing of concrete, and the yielding of the steel reinforcement. These effects are particularly difficult to incorporate in the FE analysis as they may induce highly non-linear deformations and lead to severe convergence problems when computing the numerical solution, thus, increasing the computational effort and posing significant computational challenges [11]. Therefore, incorporating detailed FE models of RC walls with non-linear material models is rarely the case for the analysis and design of buildings in the engineering practice [12]. Instead, such models are mostly used for research purposes or in highly important engineering projects.

To avoid the necessity of computationally expensive FE models in the simulation of buildings, engineers and researchers have created many safety guidelines and simplified methodologies that are usually accepted in the building design codes. For example, modeling shear walls with simple linear elastic beam or plate elements having reduced shear stiffness [13, 14]. Alternatively, more advanced modeling techniques are also gaining popularity such as the non-linear wall hinges adopted in the performance-based analysis and design [15]. Nevertheless, despite the popularity and adoption of such simplified methods, the truth is that their applicability is rather limited as they are usually unable to capture the realistic behavior of the building beyond the non-linear range, which may be surpassed during strong seismic events [12]. It is then of particularly high importance to find ways to bring the accuracy and reliability of the detailed FE models into the daily engineering design practice. An innovative way to achieve such a goal is through the implementation of Machine Learning (ML) oriented strategies. For instance, creating a data-driven surrogate model that captures the underlying physics of the problem by learning from available data [16]. The surrogate alternative model could then substitute the detailed FE counterpart, thus significantly reducing the computational effort with only small or even negligible compromise of accuracy.

With the recent developments and the ongoing research trend of ML-powered methodologies, the usage of surrogate models as substitutes for complex and computational expensive FE models has gained great popularity in many disciplines such as structural, mechanical, geotechnical, and bio-mechanical engineering [17]. In the structural engineering domain [18], Papadopoulos et al. [19] developed an artificial neural network (ANN) based surrogate beam element to analyze carbon nanotubes that is suitable for geometrically non-linear analysis. Similarly, Hau et al. [20] created a surrogate model for the geometrically non-linear analysis of truss elements using deep neural networks (DNN), and then used the surrogate model in optimization problems. Greve and van de Weg [21] proposed a ML-based strategy for creating parametric surrogate models from

parameterized finite element model simulation results. The authors used two different recurrent neural network modeling approaches for the prediction of various field quantities with different degrees of complexity and non-linearity. Hoffer et al. [22] carried out a comparative study using various FEM examples to assess the performance of various surrogate modeling strategies. They showed that ANN-based models exhibit better performance in their tested examples. In the field of dynamic analysis of structures [23], Plevris and Solorzano [24] used artificial neural networks to accurately predict the eigenperiods of multi degree of freedom (MDOF) shear buildings.

ANN-based techniques have been successfully implemented in modeling, simulating and predicting the behavior of concrete structures. Sharib et al. [25] developed an ANN-based model to estimate the load carrying capacity of RC walls directly from experimental test data. Their study shows that the predictions using the ANN-based method achieve higher accuracy than relevant formulas provided in building design codes. Solorzano and Plevris [26, 27] developed an ANN-surrogate model that was able to predict the optimum design of RC footings, reducing the computational time considerably in comparison to the mathematical models. Similar models have been successfully implemented for predicting the properties of FRP-Confined Concrete Cylinders [28], predicting the compressive strength of concrete containing recycled aggregate [29, 30], predicting the compressive strength of CRM samples [31], predicting the bond stress of corroded steel reinforcing bars in concrete members [32], determining the nominal shear capacity of steel fiber reinforced concrete beams [33], among many other interesting and innovative applications.

In this study, we develop an ANN-based surrogate model that is able to predict the lateral load capacity of a RC shear wall. This is achieved by training the model with a large database containing the results of hundreds of non-linear pushover simulations of RC shear walls with different size and properties, based on detailed FE modeling. The first part of the study focuses on the creation of the training database. To that end, we have developed an advanced parametric FE model of a RC shear wall that uses multi-layer shell elements and appropriate non-linear constitutive material laws [8]. After a successful training procedure, the surrogate model is able to learn the corresponding nonlinear structural behavior and substitute the detailed FE model.

The rest paper is organized as follows: in section 2, the basic components of a RC wall and the corresponding adopted FE model are described in detail. Then, in section 3.1, a brief introduction to the concepts of ANNs is given, following by sections 3.2 and 3.3 where a description of the implemented NN architecture and the generation of the training database are explained. In section 4, the results are presented showing the obtained correlation values of the predictions. Finally, a numerical example is given in section 4.2, followed by the conclusions of the study.

2 RC SHEAR WALL FINITE ELEMENT MODELING

2.1 RC shear wall

Reinforced concrete shear walls are essentially lateral-load-resisting elements that are commonly used in buildings to increase their lateral stiffness. They are referred to as shear walls because their main purpose is to absorb the severe shear forces that are generated when strong lateral loads are applied to the structure, such as those induced by earthquakes. They are usually an economic alternative compared to other lateral resisting systems as they also serve as columns providing support to the flooring system. An additional benefit is that shear walls can

be easily mixed into the architectural design as part of the facade or interior walls, (i.e. as the surrounding walls of the elevators, thus, providing a strong solid core to the building). Because of their importance, RC shear walls usually require special considerations in their reinforcement quantification and detailing when compared to other types of RC walls such as regular gravity-loaded RC walls.

When a building is subjected to lateral loading, the shear wall acts as a vertical cantilever beam providing additional stiffness to prevent excessive lateral displacements. As a result, at the bottom section of the wall, there is a concentration of high tensile stresses on one edge, and compression stresses on the opposite edge. Therefore, it is a common practice to provide additional reinforcement at the edges, or alternatively, increase the concrete section creating "I" shaped walls. The edges of the wall are also known as the "boundary elements" (BE) whereas the middle part of the wall is commonly referred to as "the web" and usually contains lesser quantity of steel reinforcement compared to the BE, see Figure 1.
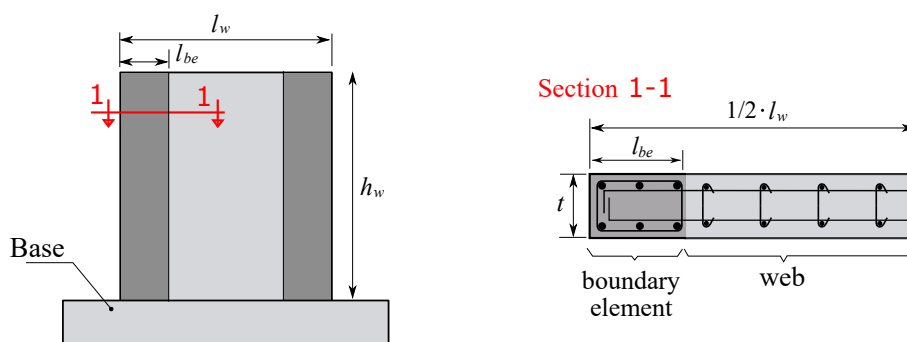

Figure 1: Components of a reinforced concrete shear wall and their corresponding notation.

2.2 Multi-layer shell element for RC walls

In this study, we adopt the RC shear wall finite element model implemented and validated by Lu et al. [34]. The model is constructed using the so-called multi-layer shell element that simplifies the 3D nonlinear behavior into a shell formulation with several fully-bonded layers in the thickness direction. Each layer may have different material properties, thus, allowing the inclusion of the reinforcement steel as smeared orthotropic layers, as shown in Figure 2.

Such multi-layer shell elements have proven effective to capture the coupled in-plane and out-of-plane bending as well as the in-plane direct shear and coupled bending/shear characteristic behavior of RC shear walls [35, 36]. By selecting a proper layer discretization, the layered-shell element is able to simulate the actual stress distribution over the thickness of the wall. Initially, the strains and the curvatures at the middle layer are computed, then, the strains in the subsequent layers are determined using the plane-section assumption. Finally, the stresses are obtained based on the corresponding constitutive law of the material of each layer.
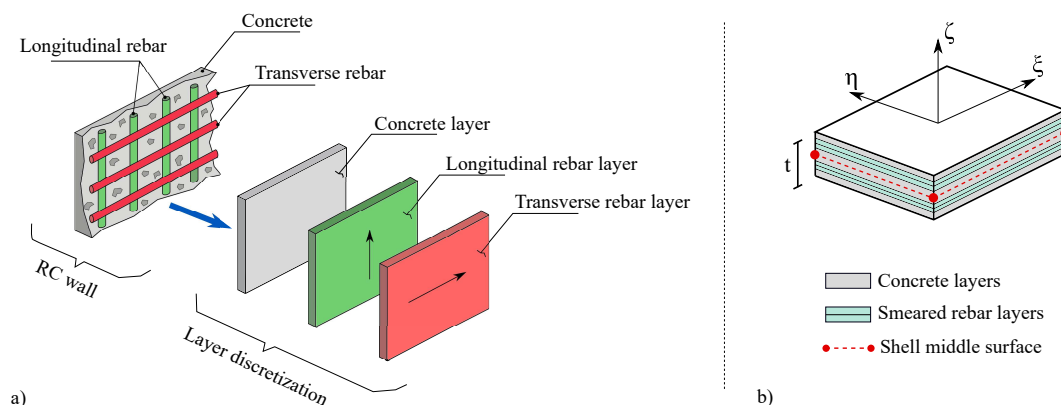
Figure 2: Multi-layer shell element: a) discretization of the reinforcement into orthotropic smeared rebar layers, b) multi-layer shell in isoparametric space.

The multi-layer shell element is implemented using the OpenSees package [37]. The base shell element is the "ShellNLDKGQ" which includes the effect of geometric non-linearity in its formulation. The layers are defined by creating a "LayeredShell" section and assigning it to the corresponding shell elements. The "LayeredShell" section contains the information of the layers which is stored as pairs of numbers, one denoting a reference to a material constitutive law and the other being the corresponding thickness value (i.e. "matA", "10", "matB", "5", "matC", "10"). The material used for the concrete layers includes the non-linear effects of cracking, crushing, and aggregate interlocking based on the damage mechanism and the smeared crack model [38]. The corresponding OpenSees implementation is the "PlaneStressUserMaterial" combined together with the "PlateFromPlaneStress" that incorporates the out-of-plane behavior. For the reinforcement steel layers, the non-linear yielding and the Bauschinger effect are considered with a uni-axial Giuffre-Menegotto-Pinto steel material formulation [39, 40]. Its implementation is the "Steel02" material in OpenSees and it is properly combined with the multi-dimensional reinforcement material "PlateRebar" so that it can be used as a shell layer.

2.3 Model description and discretization

The RC wall is modeled using the multi-layer shell element described previously. Two different layer sections are created, one used for the boundary elements (on the edges) and the other for the web (central part) of the wall. The layers for one half of the section, starting from an outer edge to the middle, are as follows: one layer for the concrete cover, then, one layer for each bed of reinforcement (longitudinal and transversal), and another two layers for the concrete core. This results in a total of 5 layers per half thickness and 10 for the whole thickness. The thicknesses of the concrete and the smeared rebar layers are computed based on the quantity of steel reinforcement of the section.

Concerning the mesh discretization, the wall is subdivided in 10 parts in the vertical direction while in the horizontal direction, the boundary elements and the web are subdivided in 2 and 4 parts, respectively. This results in a 10x8 mesh with 80 quadrilateral shell elements of approximately 20 to 40 cm in size, as illustrated in Figure 3.
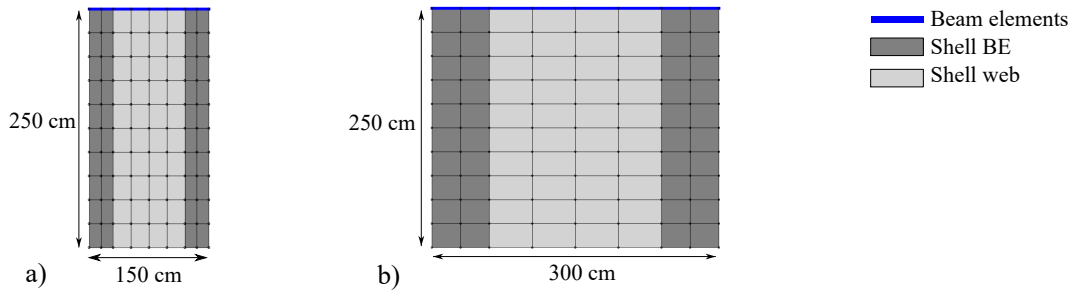
Figure 3: The adopted 10x8 shell discretization used for the RC wall model, displayed for two different wall lengths: a) 150 cm and b) 300 cm.

The model adopts the popular crack band theory [41], in which the slope of the softening branch of cracked concrete is adjusted according to the element size to eliminate the size effect. As a result, the proposed discretization should be sufficient to get accurate results as it was shown in [34], where a similar RC wall model was tested with three different mesh sizes containing 40, 160, and 360 elements, with no meaningful improvement of the results.

A horizontal beam element with a square cross section measuring $3t$ per side is included at the top of the wall. This special element serves to simulate a portion of the corresponding flooring system and to numerically stabilize the model by distributing the vertical and lateral loads to all the nodes at the top surface.

2.4 Pushover analysis

For the analysis, the wall is fixed at its base (on the bottom) and the loading is divided in two separate phases that are executed sequentially. First, the wall is subjected to a vertical compressive load P_a applied at the top-middle node, intended to simulate the loading due to gravity actions, see Figure 4a.
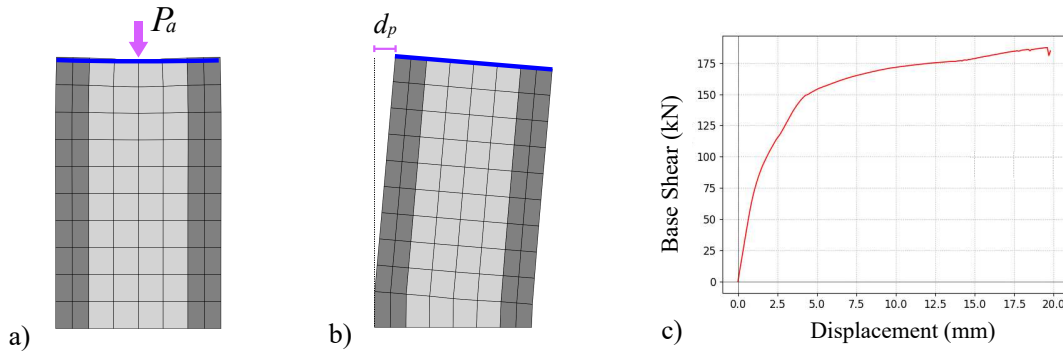

Figure 4: a) Application of the vertical load in the first step and its corresponding deformed shape (scale factor of 500). b) Applied displacement for the pushover analysis and its corresponding deformed shape (scale factor of 10). c) Pushover curve showing the characteristic force-displacement relationship.

After the gravity loading, a displacement controlled pushover analysis is performed where the wall is horizontally pushed from the top-left corner towards the right, as shown in Figure 4b. The target displacement is set to $d_p = 2$ cm with an increase of 0.005 cm for a total of $2/0.005 = 400$ steps. At each step, the horizontal reaction force at the bottom (or base shear) is calculated and stored. The typical pushover curve, which displays the force-displacement relationship, is obtained by plotting the displacement measured at the top-middle node, and the computed base shear at every step, as shown in the example of Figure 4c.

2.5 Parametric FEM model

The previously described RC shear wall model is used to create a large database of different RC walls and their corresponding pushover curves. Therefore, the model needs to be fully parameterized so that it can be analyzed multiple times with different wall sizes and other characteristics. Too many different variables would be required to fully describe the wall in detail (i.e. dimensions, material properties, steel reinforcement distribution, etc). In the present study, to keep things relatively simple and consistent, we have chosen eight variable parameters that describe the wall model. The selected parameters are the wall thickness t, the total wall length l_w, the BE length l_{be}, the longitudinal and transversal reinforcement ratios of the boundary element and the web part of the wall, denoted as $\rho_{l_{be}}$, $\rho_{t_{be}}$, $\rho_{l_{web}}$, $\rho_{t_{web}}$. The subscripts l and t denote the longitudinal and transversal directions, respectively, while be and web indicate the boundary element and the web, respectively. The last parameter is the axial load magnitude q_a that is normalized as a ratio of the ultimate compressive strength of the wall section, so that $P_a = 0.85 f'c \cdot l_w \cdot t \cdot q_a$. Table 1 shows a list of the variable parameters and their allowable lower and upper bounds for the present study. Table 2 shows a list of the constant parameters used, and their corresponding values.

Table 1: Variable parameters used for the parametric model generation.

Parameter	Lower bound	Upper bound	Description
t	12.5	25	Wall thickness [cm]
l_w	150	300	Wall length [cm]
l_{be}	$0.15 \cdot l_w$	$0.30 \cdot l_w$	BE length [cm]
$\rho_{l_{be}}$	0.01	0.035	BE long. reinf. ratio
$\rho_{t_{be}}$	0.0075	0.01	BE transv. reinf. ratio
$\rho_{l_{web}}$	0.0025	$0.5 \cdot \rho_{l_{be}}$	Web long. reinf. ratio
$\rho_{t_{web}}$	0.0025	0.0075	Web transv. reinf. ratio
q_a	0.01	0.075	Axial load ratio

Table 2: Constant parameters used for the parametric model generation.

Parameter	Value	Description
h_w	250	Wall height [cm]
r	1.25	Concrete cover [cm]
f_c'	30.8	Concrete compressive strength [MPa]
f_t	30.8	Concrete tensile strength [MPa]
f_{cu}	-6.16	Concrete crushing strength [MPa]
ϵ_{co}	-0.002	Strain at max strength
ϵ_{cu}	-0.005	Strain at crushing strength
ϵ_{tu}	0.001	Ultimate tensile strain
f_y	392	Reinf. steel yield strength [MPa]
E_0	202.7	Reinf. steel initial elastic mod. [GPa]
b	0.01	Reinf. steel strain-hardening ratio

The upper and lower bounds of the variable parameters are based on engineering experience as well as the design guidelines by the American Concrete Institute (ACI318-19) [42]. For example, the minimum thickness of a structural wall allowed is 12.5 cm, the smallest allowed length to thickness ratio for a wall is 6 (from the selected values, the minimum length and the maximum thickness equals 150/25=6), the required transversal reinforcement for the special boundary element is according to section 18.10.6.4 of the code, resulting in the chosen value of $\rho_{t_{be}}$=0.0075. Additionally, according to [2], an axial load ratio value of $q_a = 0.1$ is representative to the loading of a wall in a medium-height building. Parameters related to material properties, such as the concrete compressive strength and the steel yield stress, as well as the wall height and others, are kept constant, with their values shown in Table 2.

3 NEURAL NETWORK SURROGATE MODELING

A surrogate model is meant to substitute a complex and computationally expensive mathematical model with a simpler and faster alternative. In this study, our goal is to substitute the previously described FE model of the RC wall with an artificial neural network. The network is trained to predict the lateral load capacity of the wall which is the maximum value measured in the corresponding pushover curve. ANNs constitute an extensive topic on their own and their formulation, concepts and different applications areas in structural engineering can be found in the literature [43, 44, 45, 46, 47]. In this paper, we provide the reader only with the basic ideas in the following sections 3.1 to 3.3.

3.1 Neural Networks basics

Artificial Neural Networks are a subset of machine learning and are the basis of most modern Artificial Intelligence (AI) applications. In essence, they are predictive models that are built using large amounts of data. Their name and structure are both inspired by the human brain, particularly, in how the information is processed through big networks of interconnected neurons. Their structure consist of many nodes (or artificial neurons) that are grouped and arranged in

sequentially connected layers, so that nodes from the first layer are connected to the ones of the second layer, the ones of the second with the ones of the third, and so on, see Figure 5a. The mathematical formulation of an ANN consists of a series of weighted summations that are performed at each neuron, starting from the first layer (input layer) and propagating all the way to the last layer (output layer), see Figure 5b.
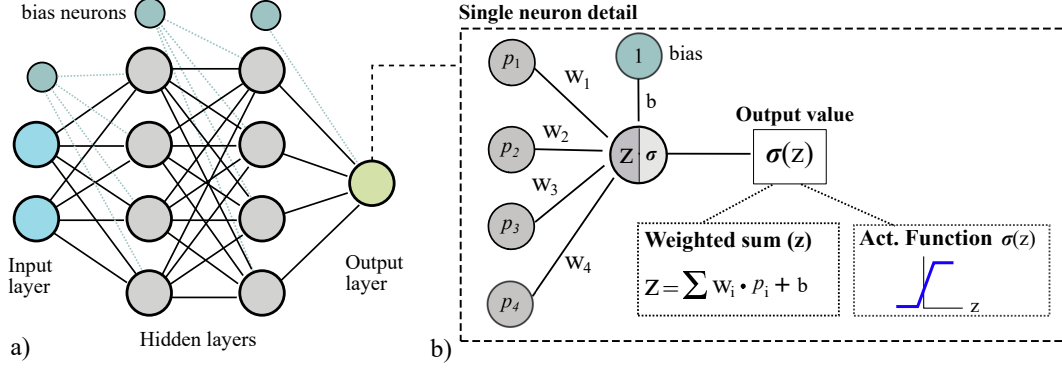

Figure 5: Artificial Neural Network graphical representation

The value of the weighted summation z, for a neuron in the layer j, is obtained as follows:

$$z = \sum_{i=1}^{n} w_i p_i + b \tag{1}$$

where n is the number of neurons at the previous layer $(j-1)$; w_i are the weights between the neurons from the $(j-1)$ and the j layer; p_i are the neuron output values from the layer $(j-1)$; and b is the bias or threshold value. The output value p of the neuron is obtained by passing the result of the weighted summation z to the neuron's activation function σ.

$$p = \sigma(z) \tag{2}$$

The activation functions are used to add non-linearity to the neural network and to facilitate the training process in which the gradient of the model parameters (i.e. the weights) must be computed. Furthermore, they add stability to the network by restricting the output values to a certain limit. Therefore, activation functions are usually simple, continuous, and differentiable functions. Two popular examples are the Sigmoid and the ReLu activation functions [26]:

$$\text{ReLu}: \quad \sigma(z) = \begin{cases} 0 & \text{for } z < 0 \\ z & \text{for } z >= 0 \end{cases} \tag{3}$$

$$\text{Sigmoid}: \quad \sigma(z) = \frac{1}{1 + e^{-z}} \tag{4}$$

The weight values represent the connection strengths between the neurons. It is by adjusting the weights that the neural network is trained and it becomes able to predict the desired output.

The process of adjusting the weights is called training. For that, a large database of known inputs and outputs is required, which is commonly known as training data. A simple description of the training procedure is the following: (1) the NN is initialized with random weights; (2) the training data is fed to the input layer, one data point at a time. For every set of input values, the corresponding output value is computed and compared with the real known output; (3) the resulting error is measured and the weights are slightly updated accordingly; (4) steps 1 to 3 are repeated numerous times until the error is significantly reduced or a termination criterion is satisfied.

If the training process is successful, the neural network should be able to provide a good approximation of the output value given the input values. Furthermore, the real advantage of the network is that it is able to predict the output even for input values that were not included in the training data (as long as the new inputs are withing the range of the training data), thus, becoming a simple yet powerful and robust multi-dimensional estimator (or interpolator).

The size of the ANN (number of layers and the number of nodes per layer) as well as the network architecture and its connectivity, depends on the type of problem to be solved and on the training data that is available. For regression problems, one of the most popular and straight forward network types is the back propagation neural network (BPNN) which is also employed in the present study. The implementation is carried out using the sequential model provided by the TensorFlow python library. The exact architecture and the network parameters used are described in the following section.

3.2 Implemented BPNN details

The implemented network architecture that is used as a surrogate model has the following architecture: 8-50-50-1. Such notation indicates that it has an input layer of 8 neurons (corresponding to the 8 variable parameters of the parametric model), 2 hidden layers with 50 neurons each, and one output layer with a single neuron. A fully connectivity among the layers is considered that results in a total number of trainable parameters (or weights) of $[(8 + 1) \cdot 50] + [(50 + 1) \cdot 50] + [(50 + 1) \cdot 1] = 3051$ (the +1 indicates the bias neuron that is added to each layer). For the training phase, the selected error metric is the mean squared error (MSE) and the weight optimization algorithm is the stochastic gradient descent (SGD). The data is randomly split into two sets, one for validation using 20% of the total data, and one for the training using the remaining 80%. Additionally, a batch size of 5 is used, meaning that the weights are updated every time that 5 data points are fed to the network. The maximum number of epochs is set to 200. In addition, to avoid over-training, an early stop is enforced if it is observed that the error of the validation set is higher than the one of the training set in 10 sequential epochs.

3.3 Training database

The training database for the ANN-based surrogate model contains 1000 data points that correspond to the pushover analysis of 1000 shear walls with different parameters using the parametric model described in section 2. Each data point has 8 input values and 1 output value. The inputs values correspond to the 8 variables described in section 2.5. The database is created by randomly generating the 1000 sets of input values using a uniform distribution

in accordance with the lower and upper bounds shown in Table 1. The output value in each case is the maximum base shear force, or in other words, the maximum value obtained from the pushover curve.

4 RESULTS

The ANN is trained using the architecture described in section 3.2, and the database detailed in section 3.3. The progression of the training is shown by plotting the computed error (MSE value) for both the training and the validation sets at the end of every epoch, as shown in Figure 6. The output values obtained with the ANN are known as the "predictions" and are denoted as $\mathbf{p} = \{p_1, ..., p_n\}$. Similarly, the output values that are read from the database are referred as "real", "true", or the "ground truth" values, and are indicated as $\mathbf{r} = \{r_1, ..., r_n\}$.
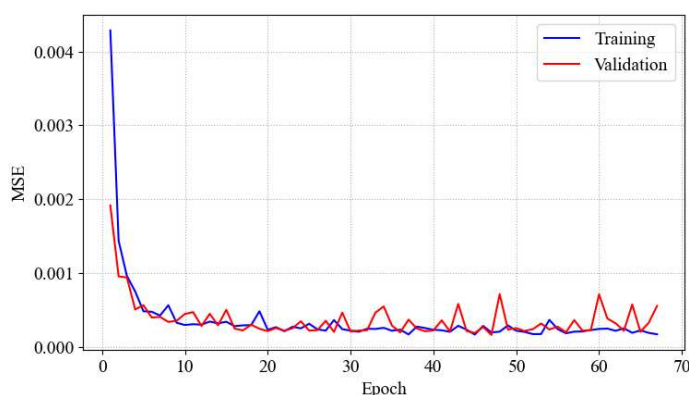

Figure 6: Mean squared error history plot for the training and validations sets.

4.1 Testing and Validating the ANN

The ANN is tested to confirm that the training procedure has been successful. This is achieved by first feeding the training input values to the network, then, computing their corresponding predictions and measuring their correlation. The real output data and the corresponding predictions are plotted as points with the form $q_i = \{r_i, p_i\}$ in Figure 7a. The vertical distance of any point q_i to the $x = y$ line (plotted in red), denotes the error of the prediction with respect to the real value. The Pearson correlation coefficient (R) and the Coefficient of Determination (R^2) are also computed and displayed in the plot. The obtained correlation values $R = 0.99814$, and $R^2 = 0.99625$, indicate that the surrogate model works very well for predicting the training data, thus, confirming that the training process has been successful. A histogram showing the error distribution is plotted in Figure 7b.

The next step is to validate the network with values that are not included in the training database, to ensure that the ANN has not been over-fitted during the training and can exhibit generalization capabilities. To that end, an additional database of 50 new points is generated using the procedure described in 3.3. The new data set is then fed to the network and the

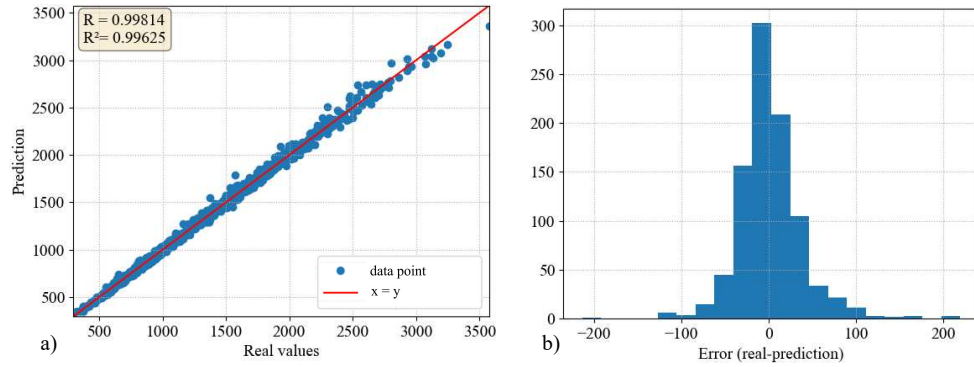corresponding outputs are computed. The results are shown in Figure 8.

Figure 7: a) Correlation between the real and the predicted values using the training database. b) Error distribution using the training database. Units in kN for both plots.
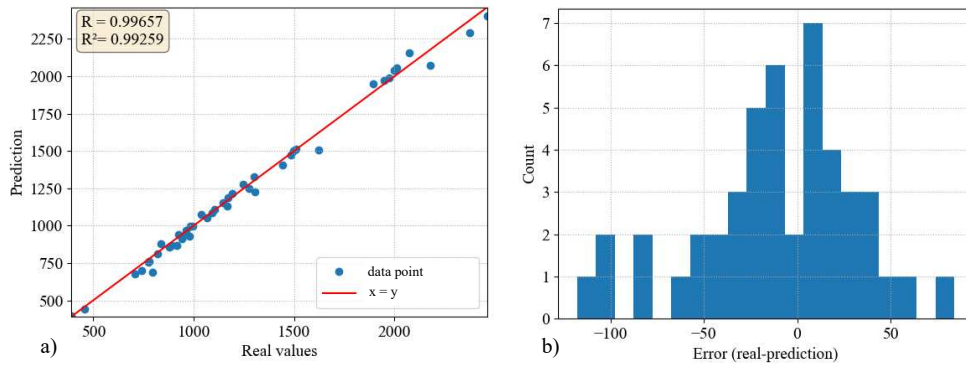

Figure 8: a) Correlation between the real and the predicted values using the testing database. b) Error distribution using the testing database. Units in kN for both plots.

The obtained correlation values for the new testing database are $R = 0.99657$, and $R^2 = 0.99259$. Furthermore, the mean squared error obtained is $MSE = 1596.3660$, which translates into an average error of $\sqrt{1596.3660} = \pm 39.95$ kN. Therefore, the results suggest that the developed ANN-based surrogate model has captured the underlying physics of the problem and is able to predict the lateral load capacity of the RC wall with an estimated average error of ± 39.95 kN. It is important to keep in mind that the results are only valid if the input values are inside the lower and upper bounds specified in Table 2.5. The greatest advantage of the developed surrogate model is the reduction in the time required to compute the solution. The pushover analysis using the detailed FEM model of the RC wall can take up to 60 seconds (for 400 steps) to perform, while the trained ANN computes the output in less than 5 milliseconds. These computation times are measured on a regular PC with an Intel Core i7-6700HQ CPU

@2.60GHz and 8 GB RAM. In the ANN-based surrogate approach, the most computationally expensive part of the methodology is related to the generation of the training database, which in this case required the computation of 1000 FE simulations. However, it is a single-time process (needed to be done only once). The training of the ANN itself is a faster procedure which also needs to be executed only once. After these two time-consuming phases have been completed, the ANN is ready to be stored and further used for any other simulation, providing new results at lightning speed.

4.2 Numerical example

A numerical example is carried out as a means to visualize the problem in terms of engineering values. The selected input values for the example are the following: $t = 20$ cm, $l_w = 200$ cm, $l_{be} = 50$ cm, $\rho_{l_{be}} = 0.03$, $\rho_{t_{be}} = 0.0075$, $\rho_{l_{web}} = 0.0030$, $\rho_{t_{web}} = 0.0030$, $q_a = 0.065$. The rest of the parameters for the model are set according to Table 2. The computed output value using the ANN-based surrogate model is $p = 1277.058$ kN, and the value obtained from the pushover analysis with the detailed FEM model is $r = 1294.39$ kN. The prediction error is therefore: $r - p = 1294.39 - 1277.058 = 17.332$ kN (or 1.34% in relative terms). The mesh of the wall, the computed pushover curve, and the predicted value for the specific shear wall are shown in Figure 9.
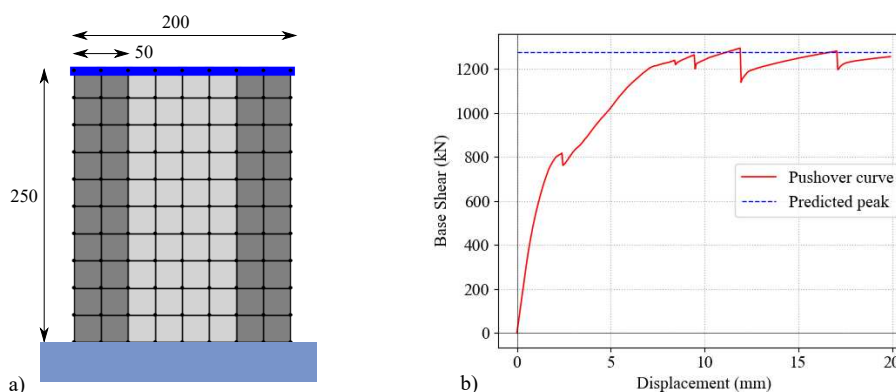

Figure 9: Numerical example. a) Mesh and dimensions of the analyzed RC wall (units in cm). b) Pushover curve obtained with the detailed FEM model and the prediction computed with the developed ANN-based surrogate model.

5 CONCLUSIONS

In this study an ANN-based surrogate model has been developed which manages to reliably predict the lateral load capacity of RC shear walls with accuracy similar to the one obtained with detailed non-linear FE pushover analysis. The most computationally expensive operations involved in the numerical procedure are (i) the creation of the database that is required for the proper training of the ANN model, and (ii) the following training of the ANN model itself. Then, after the ANN surrogate model has been properly trained, it can be used to completely substitute the FE model, thus drastically reducing the required computational time to a matter

of a few milliseconds with small compromise of accuracy. Eight variable parameters have been included in the model for describing the shear wall structure, having to do with the dimensions of the wall, the reinforcement ratios and the axial load magnitude. Other important model parameters, such as the compressive strength of concrete and the steel yield stress have been kept constant throughout the study. Although this may pose a limitation in the applicability of the methodology in real world engineering problems, we believe that the addition of these extra parameters is in fact only a technicality and can be easily done in the framework of the described methodology without any significant changes other than the ones having to do with the size and complexity of the ANN model. The expansion of the ANN model with these extra input parameters together with the possible inclusion of some additional output parameters, is an interesting topic of future research for the authors.

REFERENCES

[1] Avigdor Rutenberg. Seismic shear forces on RC walls: review and bibliography. *Bulletin of Earthquake Engineering*, 11(5):1727–1751, October 2013.

[2] Ioannis Lefas and Michael Kotsovos. Behavior of reinforced concrete structural walls. Strength, deformation characteristics, and failure mechanism. *ACI Structural Journal*, 87:23–31, January 1990.

[3] R.G Oesterle, A.E. Fiorato, H.G. Russell, and W.G. Corley. Earthquake Resistant Structural Walls - Test of Isolated Walls Phase II. Technical report, Construction Technology Laboratories, California, USA, October 1979.

[4] X.L. Lu, Y. Zhou, J.H. Yang, J. Qian, C. Song, and Y. Wang. SLDRCE Database on Static Tests of Structural Members and Joint Assemblies - Shear walls R11. Technical report, Institute of Structural Engineering and Disaster Reduction, Tongji University, Shanghai, China, Shanghai, China, 2008.

[5] Vincenzo Colotti. Shear Behavior of RC Structural Walls. *Journal of Structural Engineering*, 119(3):728–746, March 1993. Publisher: American Society of Civil Engineers.

[6] Seong-Hoon Jeong and Won-Seok Jang. Modeling of RC shear walls using shear spring and fiber elements for seismic performance assessment. *Journal of Vibroengineering*, 18:1052–1059, March 2016.

[7] Xilin Lu and Yuntao Chen. Modeling of Coupled Shear Walls and Its Experimental Verification. *Journal of Structural Engineering-asce - J STRUCT ENG-ASCE*, 131, January 2005.

[8] Linlin Xie, Xiao Lu, Xinzheng Lu, Yuli Huang, and Lieping Ye. *Multi-Layer Shell Element for Shear Walls in OpenSees*. June 2014. Pages: 1197.

[9] İlker Kazaz, Ahmet Yakut, and Polat Gülkan. Numerical simulation of dynamic shear wall tests: A benchmark study. *Computers & Structures*, 84:549–562, March 2006.

[10] Jordlly Silva and Bernardo Horowitz. Nonlinear finite element analysis of reinforced concrete shear walls. *Revista IBRACON de Estruturas e Materiais*, 13, January 2020.

[11] Vagelis Plevris and George C. Tsiatas. Computational structural engineering: Past achievements and future challenges. *Frontiers in Built Environment*, 4, 2018.

[12] NICOLAE ILE* and J. M. REYNOUARD†. Nonlinear Analysis of Reinforced Concrete Shear Wall Under Earthquake Loading. *Journal of Earthquake Engineering*, 4(2):183–213, April 2000. Publisher: Taylor & Francis _eprint: https://doi.org/10.1080/13632460009350368.

[13] Tang T.O. and R.K.L. Su. Shear and Flexural Stiffnesses of Reinforced Concrete Shear Walls Subjected to Cyclic Loading. *The Open Construction and Building Technology Journal*, 8:104–121, July 2014.

[14] Xiangyong Ni, Shuangyin Cao, Yizhu Li, and Shuai Liang. Stiffness degradation of shear walls under cyclic loading: experimental study and modelling. *Bulletin of Earthquake Engineering*, 17, September 2019.

[15] Garrett Hagen. Performance-Based Analysis of a Reinforced Concrete Shear Wall Building. June 2012.

[16] S.E. Gano, H. Kim, and D.E. Brown II. Comparison of three surrogate modeling techniques: Datascape®, kriging, and second order regression. volume 3, pages 1690–1707, 2006.

[17] Poojitha Vurtur Badarinath, Maria Chierichetti, and Fatemeh Davoudi Kakhki. A Machine Learning Approach as a Surrogate for a Finite Element Analysis: Status of Research and Application to One Dimensional Systems. *Sensors (Basel, Switzerland)*, 21(5):1654, February 2021.

[18] Nikolaos D. Lagaros and Manolis Papadrakakis. Learning improvement of neural networks used in structural optimization. *Advances in Engineering Software*, 35(1):9–25, 2004.

[19] V. Papadopoulos, G. Soimiris, D. G. Giovanis, and M. Papadrakakis. A neural network-based surrogate model for carbon nanotubes with geometric nonlinearities. *Computer Methods in Applied Mechanics and Engineering*, 328:411–430, January 2018.

[20] Hau T. Mai, Joowon Kang, and Jaehong Lee. A machine learning-based surrogate model for optimization of truss structures with geometrically nonlinear behavior. *Finite Elements in Analysis and Design*, 196:103572, November 2021.

[21] Lars Greve and Bram Pieter van de Weg. Surrogate modeling of parametrized finite element simulations with varying mesh topology using recurrent neural networks. *Array*, 14:100137, July 2022.

[22] Johannes G. Hoffer, Bernhard C. Geiger, Patrick Ofner, and Roman Kern. Mesh-Free Surrogate Models for Structural Mechanic FEM Simulation: A Comparative Study of Approaches. *Applied Sciences*, 11(20):9411, January 2021. Number: 20 Publisher: Multidisciplinary Digital Publishing Institute.

[23] George Papazafeiropoulos and Vagelis Plevris. Openseismomatlab: A new open-source software for strong ground motion data processing. *Heliyon*, 4(9), 2018.

[24] Vagelis Plevris and German Solorzano. Prediction of The Eigenperiods of MDOF Shear Buildings using Neural Networks. In *8th International Conference on Computational Methods in Structural Dynamics and Earthquake Engineering*, pages 3894–3911, Streamed from Athens, Greece, 2021. ECCOMAS Proceedia.

[25] S. Sharib, N. Ahmad, Vagelis Plevris, and A. Ahmad. Prediction models for load carrying capacity of rc wall through neural network. In *14th International Conference on Evolutionary and Deterministic Methods for Design, Optimization and Control*, pages 132–142, Athens, Greece, 2021.

[26] German Solorzano and Vagelis Plevris. Design of Reinforced Concrete Isolated Footings under Axial Loading with Artificial Neural Networks. In *14th ECCOMAS Thematic Conference on Evolutionary and Deterministic Methods for Design, Optimization and Control (EUROGEN 2021)*, pages 118–131, Streamed from Athens, Greece, 2021. ECCOMAS Proceedia.

[27] German Solorzano and Vagelis Plevris. Optimum Design of RC Footings with Genetic Algorithms According to ACI 318-19. *Buildings*, 10(6):110, June 2020. Number: 6 Publisher: Multidisciplinary Digital Publishing Institute.

[28] Afaq Ahmad, Vagelis Plevris, and Qaiser-uz-Zaman Khan. Prediction of properties of frp-confined concrete cylinders based on artificial neural networks. *Crystals*, 10(9), 2020.

[29] Hamed Dabiri, Mahdi Kioumarsi, Ali Kheyroddin, Amirreza Kandiri, and Farid Sartipi. Compressive strength of concrete with recycled aggregate; a machine learning-based evaluation. *Cleaner Materials*, 3:100044, 2022.

[30] Amirreza Kandiri, Farid Sartipi, and Mahdi Kioumarsi. Predicting compressive strength of concrete containing recycled aggregate using modified ann with different optimization algorithms. *Applied Sciences*, 11(2), 2021.

[31] M I Waris, J Mir, V Plevris, and A Ahmad. Predicting compressive strength of CRM samples using image processing and ANN. *IOP Conference Series: Materials Science and Engineering*, 899(1):012014, jul 2020.

[32] Masoud Ahmadi, Ali Kheyroddin, and Mahdi Kioumarsi. Prediction models for bond strength of steel reinforcement with consideration of corrosion. *Materials Today: Proceedings*, 45:5829–5834, 2021. Second International Conference on Aspects of Materials Science and Engineering (ICAMSE 2021).

[33] Masoud Ahmadi, Ali Kheyroddin, Ahmad Dalvand, and Mahdi Kioumarsi. New empirical approach for determining nominal shear capacity of steel fiber reinforced concrete beams. *Construction and Building Materials*, 234:117293, 2020.

[34] Xinzheng Lu, Linlin Xie, Hong Guan, Yuli Huang, and Xiao Lu. A shear wall element for nonlinear seismic analysis of super-tall buildings using OpenSees. *Finite Elements in Analysis and Design*, 98, June 2015.

[35] Philip Hallinan and Hong Guan. Layered Finite Element Analysis of One-Way and Two-Way Concrete Walls with Openings. *Advances in Structural Engineering*, 10(1):55–72, February 2007. Publisher: SAGE Publications Ltd STM.

[36] Hong Guan and Yew-Chaye Loo. Flexural and Shear Failure Analysis of Reinforced Concrete Slabs and Flat Plates. *Advances in Structural Engineering*, 1(1):71–85, January 1997. Publisher: SAGE Publications Ltd STM.

[37] Frank McKenna, Michael H. Scott, and Gregory L. Fenves. Nonlinear Finite-Element Analysis Software Architecture Using Object Composition. *Journal of Computing in Civil Engineering*, 24(1):95–107, January 2010. Publisher: American Society of Civil Engineers.

[38] A. Hillerborg, M. Modéer, and P.-E. Petersson. Analysis of crack formation and crack growth in concrete by means of fracture mechanics and finite elements. *Cement and Concrete Research*, 6(6):773–781, 1976.

[39] M. Menegotto. Method of analysis of cyclically loaded RC plane frames including changes in geometry and non-elastic behavior of elements under normal force and bending. *undefined*, 1973.

[40] Filip C Filippou, E. P Popov, and Vitelmo V Bertero. Effects of bond deterioration on hysteretic behavior of reinforced concrete joints. Technical report, Earthquake Engineering Research Center, University of California, Berkeley, California, 1983. OCLC: 654724602.

[41] Zdeněk P. Bažant. Size Effect in Blunt Fracture: Concrete, Rock, Metal. *Journal of Engineering Mechanics*, 110(4):518–535, April 1984. Publisher: American Society of Civil Engineers.

[42] ACI Committee 2019. *ACI 318-19 Building Code Requirements for Structural Concrete.* Farmington Hills, MI, 2019.

[43] Vagelis Plevris. *Innovative Computational Techniques for the Optimum Structural Design Considering Uncertainties*. PhD thesis, National Technical University of Athens, 2009.

[44] Panagiotis G. Asteris and Vagelis Plevris. Neural network approximation of the masonry failure under biaxial compressive stress. In *3rd South-East European Conference on Computational Mechanics (SEECCM III)*, pages 584–598, Kos Island, Greece, 2013. ECCOMAS Proceedia.

[45] Vagelis Plevris and Panagiotis G. Asteris. Modeling of masonry compressive failure using neural networks. In *OPT-i 2014 An International Conference on Engineering and Applied Sciences Optimization*, pages 2843–2861, Kos Island, Greece, 2014.

[46] Vagelis Plevris and Panagiotis G. Asteris. Anisotropic failure criterion for brittle materials using artificial neural networks. In *5th International Conference on Computational Methods in Structural Dynamics and Earthquake Engineering (COMPDYN 2015)*, pages 2259–2272, Crete Island, Greece, 2015. ECCOMAS Proceedia.

[47] Nikos D. Lagaros and Manolis Papadrakakis. Neural network based prediction schemes of the non-linear seismic response of 3d buildings. *Advances in Engineering Software*, 44(1):92–115, 2012. CIVIL-COMP.